Dissociation, ionization, and Coulomb explosion of H_2^+ in an intense laser field by numerical integration of the time-dependent Schrödinger equation

Szczepan Chelkowski,[1] Tao Zuo,[1] Osman Atabek,[2] and André D. Bandrauk[1]
[1]*Laboratoire de Chimie Théorique, Faculté des Sciences, Université de Sherbrooke, Sherbrooke, Québec, Canada J1K 2R1*
[2]*Laboratorie de Photophysique Moléculaire, Batiment 213, Université Paris-Sud, 91405 Orsay, France*
(Received 20 March 1995)

The time-dependent Schrödinger equation for H_2^+ in a strong laser field is solved numerically for a model that uses the exact three-body Hamiltonian with one-dimensional nuclear motion restricted to the direction of the laser electric field. The influence of ionization on possible stabilization against dissociation is investigated. Unexpectedly high ionization rates from high vibrational states, exceeding those of neutral atomic hydrogen, are found. The ionization rates as functions of the internuclear distance R were also calculated for fixed nuclei, and these exhibit two strong maxima at large R, which explain the full dynamical results. A series of peaks seen in the calculated proton energy spectra can therefore be interpreted as occurring preferentially at (i) turning points of laser-induced vibrationally trapped states, and (ii) at the ionization maxima that occur at large internuclear distances of H_2^+.

PACS number(s): 42.50Hz, 33.80Rv, 34.50 Gb, 35.80+s

I. INTRODUCTION

The interaction of intense laser pulses (intensity $>10^{13}$ W/cm^2) with atoms and molecules has been an area of active studies during the past two decades [1–4]. One of the theoretical approaches to deal with this nonperturbative problem relies on exact numerical solutions of the time-dependent Schrödinger equation (TDSE) on recently available supercomputers [3–7]. So far this approach has been successfully applied to simple atoms [3,4] or molecules with frozen nuclei [5–7]. Most of the theoretical work for molecules in strong fields is restricted to the use of several lowest or essential electronic states, giving rise to a dressed-state interpretation [2]. This paper is an attempt to go beyond the previous approaches by including both electronic and nuclear degrees of freedom. Moreover, our approach goes beyond the Born-Oppenheimer approximation. We are motivated first by the fact that there is a lot of interest in the phenomenon of suppression of resonant dissociation of H_2^+ by an intense laser pulse [2,8–11]. This process is typically described as a model in which only the ground-state electronic surface and the first repulsive surface are included [2,8–11] (i.e., ionization and coupling to upper electronic surfaces are neglected). Therefore it is important to know up to what laser intensities are predictions of the two-electronic-state model valid. One of the predictions of this model based on dressed-state representation is the very interesting phenomenon of laser-induced molecular stabilization with respect to the dissociation at high laser intensities by the mechanism of *laser-induced avoided crossings* [2,8,9]. We wish to examine the extent to which ionization may affect this stabilization.

Second, there are new experiments on Coulomb explosions of small molecules in intense laser fields [13]. For such experiments the electron-nuclear dynamics must be considered concurrently. The present calculations are an attempt to address this question.

II. MODEL

In this paper we extend our previous studies of ionization of H_2^+ with intense lasers [6,7]. While previously the nuclear motion was frozen, we allow here one-dimensional (1D) motion of the nuclei along the polarization direction of the electric-field vector of the linearly polarized radiation. The electron is allowed to move in three dimensions. Because of the cylindrical symmetry of such a model, here we deal with three spatial degrees of freedom, ρ, z, and R, where ρ and z are electron cylindrical coordinates with respect to the molecular center of mass and R is the internuclear distance, with both z and R along the direction of the electric field. In these coordinates the TDSE for this three-body system (after the elimination of the center-of-mass motion) has the following form [14]:

$$i\hbar\frac{\partial\psi}{\partial t}=\left(-\beta\frac{\partial^2}{\partial z^2}-\beta D_\rho+T_R+V(\rho,z,R)+e\kappa zE(t)\right)\psi, \tag{1}$$

where

$$D_\rho=\frac{\partial^2}{\partial\rho^2}+\frac{1}{\rho}\frac{\partial}{\partial\rho}, \tag{2}$$

$$V_c(\rho,z,R)=\frac{e^2}{R}-\frac{e^2}{[\rho^2+(z-R/2)^2]^{1/2}}-\frac{e^2}{[\rho^2+(z+R/2)^2]^{1/2}}, \tag{3}$$

$$\beta=\frac{\hbar^2(2m_p+m_e)}{4m_pm_e},\quad T_R=\frac{-\hbar^2\partial^2}{m_p\partial R^2},\quad \kappa=1+\frac{m_e}{2m_p+m_e}, \tag{4}$$

and m_e, m_p are electron and proton masses. The Hamiltonian in (1) is the exact three-body Hamiltonian (obtained after separation of the center-of-mass motion), which we took from the formula (II.2) from Ref. [14]. The only ap-

TABLE I. Values of parameters used in calculations.

I W/cm^2	ω (a.u.)	z_I (a.u.)	$z_{\max}$ (a.u.)	$R_{\max}$ (a.u.)	L (a.u.)	Δt
3.5×10^{13}	0.21	32	32	24	8	0.01
10^{14}	0.21	32	96	32	8	0.01

proximation that was done consists of neglecting molecular rotations by restricting the nuclei to move only along the polarization vector of the electronic field. This seems to be a reasonable approximation since there exists ample experimental [12] and theoretical [9,10] evidence of alignment of molecular ions in strong laser fields. This is consistent with the fact that the molecular rotation time scale is much larger than the 20-fs time scale for ionization and dissociation at intensities above 10^{13} W/cm^2. Thus initial rotational pumping of H_2 is expected to occur prior to ionization, resulting in laser-aligned H_2^+ molecules. This is the starting point of our calculations. Note that there are no terms depending on angle φ in (1). These terms can be omitted due to the symmetry of this problem (the potentials and wave function at $t=0$ do not depend on φ) for aligned molecules.

The time-dependent Schrödinger equation (1) was integrated numerically with the help of the Bessel-Fourier expansion [6] in the ρ variable. This allows us to eliminate the singularities present in the Laplacian and in the potential and to use a split operator technique together with fast Fourier transform (FFT) [6,14] in the electron z and nuclear R variables. For more details about the numerical procedure used in this paper we refer the reader to our previous paper [6,15]. In the present paper, a straightforward generalization of the previously described method, to include R, R being the nuclear degree of freedom, is used. As an initial condition we used $\psi(\rho,z,R,t)=\psi_6(\rho,z,R)$ at $t=0$ equal to the product of the $1\sigma_g$-state electronic wave function of H_2^+ and the $v=6$ vibrational excited-state wave function $\varphi_6(R)$. We chose this particular vibrational state since we showed previously that for the laser wavelength $\lambda=212$ nm, strong *molecular stabilization* [2,9] occurs due to vibrational trapping by laser-induced avoided crossing between the $1\sigma_g$ and $1\sigma_u$ electronic surfaces. The radius of the grid cylinder in ρ was $L=8$ bohrs, and 16 basis functions were used in the Bessel-Fourier series. The time step δt was 0.01 a.u.$=2.4\times10^{-4}$ fs. The grid for the nuclear R variable was defined by 0.38 bohr $<R<R_{\max}$ with the size of integration step $\Delta R=\frac{1}{12}$ bohr. The size of the electron grid was defined by $|z|<z_{\max}$, with the integration step $\Delta z=\frac{1}{8}$ bohr. An absorbing mask function [4] was used to avoid the electron reflections from the boundary $|z|=z_{\max}$. Since the protons are much slower than the electron, no absorber was necessary at the proton boundary $R=R_{\max}$. The electric field was described by the formula $E(t)=E_0U(t)\sin(\omega t)$, where $U(t)=1$ for $t>t_0$, $U(t)=t/t_0$ for $0<t<t_0$, $\omega=0.21$ a.u. ($\lambda=212$ nm), $t_0=1$ fs, and E_0 is the laser peak electric field. The values of all these parameters used in our calculations are listed in Table I.

We calculated several joint probabilities, $P_D(t)$, $P_I(t)$, $f_1(R,t)$, $f(R,t)$, of finding the electron and protons in specific regions in space, which illustrate the time evolution of the system. These are defined by the formulas

$$P_D=\text{Prob}(R>R_D \text{ and } |z|<z_I), \tag{5}$$

where R_D is the range of attractive interatomic forces. We took $R_D=9.5$ bohrs, as in our previous work [10], for the calculation of dissociation probabilities. The H_2^+ $1\sigma_u$ potential flattens visibly near $R=R_D$, and its value is very close to the dissociation energy. Thus P_D can be written in the following form:

$$P_D(t)=\int_{R_D}^{R_{\max}} f_1(R,t)dR,$$

where

$$f_1(R,t)=\int_0^L d\rho\rho\int_{-z_I}^{z_I} dz|\psi|^2. \tag{6}$$

P_D is the joint probability of finding the electrons in $|z|<z_I$ and protons in $R_D<R<R_{\max}$. In all of our calculations we used $z_I=32$ a.u., while $R_{\max}$ and $z_{\max}$ were different for different intensities; see Table I. The function $f_1(R,t)$ is the joint probability density of finding the protons at the distance R and the electron within the area defined by $|z|<z_I$. We also calculated

$$P_I=\text{Prob}(z>|z_I|)=1-\int_0^{R_{\max}} dRf_1(R,t). \tag{7}$$

Thus P_I is the probability of finding the electron outside the cylinder volume defined by $|z|<z_{\max}=32$ bohrs, i.e., in the area still far from each of the protons (even at the end of our pulses the protons are very close to their c.m., $R/2<12$ a.u.). Therefore, in our model, P_I is a measure of ionization, i.e., probability for the channel $H^+ + H^+ + e^-$, while P_D is a measure of dissociation into $H+H^+$ in the presence of electrons near one of the protons ($z<|z_I|$ and $R>R_D$). We use this last quantity when comparing with two-surface calculations, which obviously include only the channel $H+H^+$. For the higher laser intensity $I=10^{14}$ W/cm^2 we used a much larger box for the electron, $z_{\max}=96$ a.u. For this case we also calculated the total function $f(R,t)$, i.e., the proton distribution function, with electrons within $|z|<z_{\max}$,

$$f(R,t)=\int_0^L d\rho\ \rho\int_{-z_{\max}}^{z_{\max}} dz|\psi|^2. \tag{8}$$

Since the functions f and f_1 are obtained through integration over electronic positions, they are not normalized to one for later times because of the outgoing electron flux (the absorber was introduced at $|z|=z_{\max}$). Current computational facilities do not allow for calculating the total wave function with larger grids using full three-dimensional simulations, including both electronic and nuclear degrees of freedom. For the intensity $I=10^{14}$ W/cm^2, when we limit ourselves to $z_{\max}=3z_I$, the distribution $f_1(R)$ contains mainly H and H^+, while $f(R)$ includes much more $H^+ + H^+$ fragments, but obviously not all of them, since at $t=26$ fs 55% of these are already missing (the calculated norm of the wave function is then 0.45).

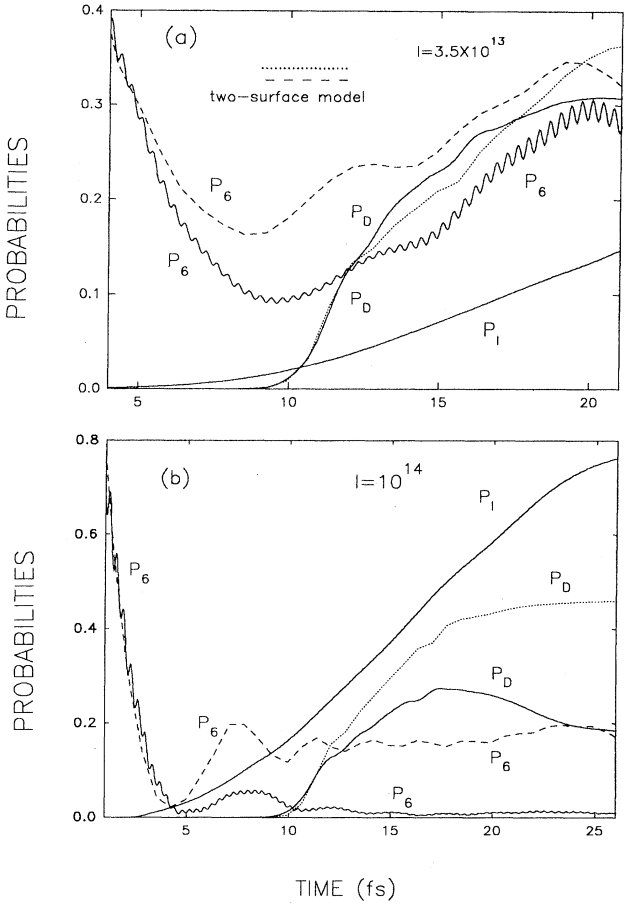

FIG. 1. Time dependence of the dissociation probability P_D, the ionization P_I, and the population P_6 of the initial $v=6$ state for intensities (a) $I=3.5\times10^{13}$ and (b) $I=10^{14}$ W/cm^2. ——, P_D from the present three-body calculations; · · · ·, two-surface calculations of P_D; -----, two-surface calculations of P_6.

Finally, we calculated the momentum Fourier transform with respect to the R variable of the outgoing proton part of the wave function in the asymptotic dissociation region ($R>R_D$), for each ρ and z value ($|z|<z_{\max}$). This gives the nuclear momentum k distribution for fixed z and ρ, from which the nuclear kinetic-energy spectra were calculated by integrating the square of the absolute value of this transform over all ρ and z values, $\rho<L$ and $|z|<z_{\max}$.

III. RESULTS AND DISCUSSION

We display in Figs. 1(a) and 1(b) the probability of dissociation P_D, ionization P_I, and the population of the initial state P_6 as functions of time for laser intensities $I=3.5\times10^{13}$ and 10^{14} W/cm^2, respectively. Previous two-surface calculations showed that *stabilization* occurs for these two intensities for the $v=6$ initial vibrational level [9] as a result of coincidence of diabatic (zero field) and adiabatic (dressed) vibrational levels. However, our results show, in Fig. 1(b) that for $I=10^{14}$ W/cm^2 the ionization process already dominates P_D and thus the stabilization phenomenon will not occur: the initial vibrational state is already almost completely

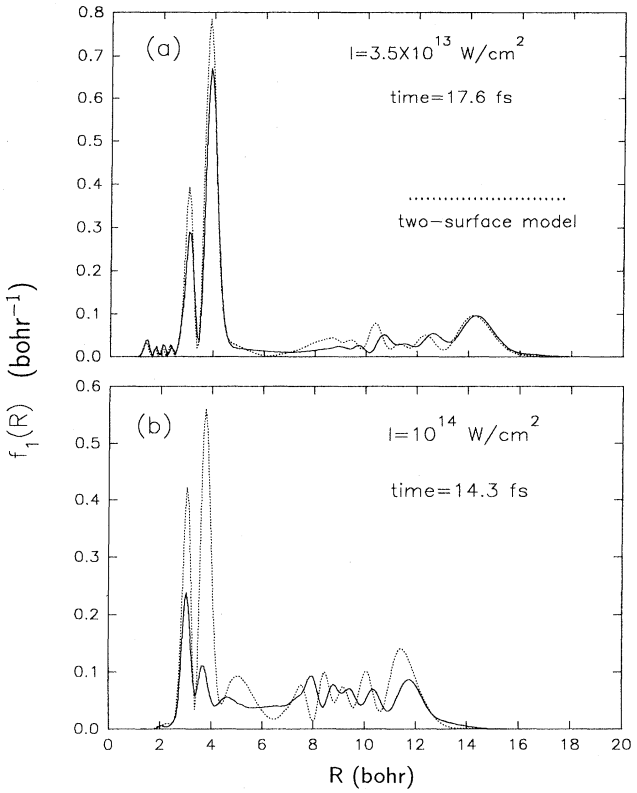

FIG. 2. Probability density $f_1(R)$ of finding the protons in R and the electron at $|z|<z_I$ a.u. for (a) $I=3.5\times10^{13}$ W/cm^2, time $=17.6$ fs, and for (b) $I=10^{14}$ W/cm^2, time$=14.3$ fs. Peaks occur at turning points of laser-induced adiabatic wells.

depopulated at 17 fs, whereas for the intensity $I=3.5\times10^{13}$ W/cm^2, Fig. 1(a), we observe the growth of P_6 up to 0.27 at 20 fs due to stimulated emission from the dissociative $1\sigma_u$ state. Note that ionization processes represented by P_I in Fig. 1 are very fast (on the molecular time scale); one sees a considerable ionization in one vibrational cycle equal to $2\pi/\omega_e$, 14.3 fs, where $\omega_e=2321$ cm^{-1} is the vibrational constant of H_2^+. The dissociation is also seen in this time scale, since the one-photon dissociated products are faster than vibrating protons (they achieve asymptotically 4.58 eV) and the transfer of population from the $1\sigma_g$ to the $1\sigma_u$ surface already occurs in this time period [9] at intensities above 10^{13} W/cm^2. The small oscillations of P_6 seen in Fig. 1 have twice the laser frequency. Such oscillations of initial-state populations are typical and present in published numerical simulations [1] (first-order "counterrotating" oscillations).

Figures 2(a) and 2(b) show the probability density $f_1(R,t)$ of finding protons at a distance R and electrons still close to them, $|z|<z_I=32$ bohrs, at fixed time values (17.6 and 14.3 fs) and Figs. 3(a) and 3(b) show the corresponding energy spectra of dissociating products also calculated for the same time. We note that both proton probability distributions $f_1(R)$ and $f(R)$ do not reach the boundaries for the times chosen, thus avoiding the necessity of introducing the absorber in the R coordinate. In Figs. 2 and 3 we show the results for two intensities, $I=3.5\times10^{13}$ and $I=10^{14}$

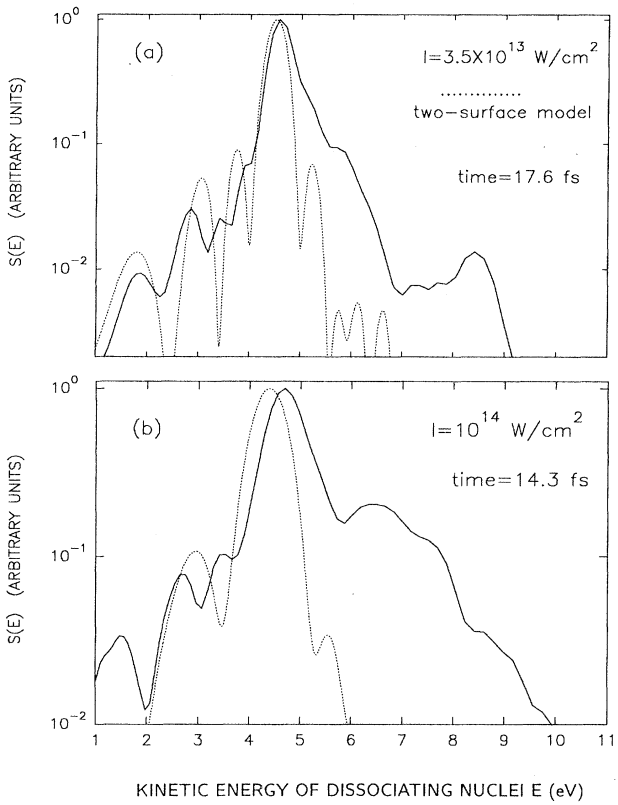

FIG. 3. Kinetic-energy spectra of outgoing protons for (a) $I=3.5\times10^{13}$ W/cm^2 at time=17.6 fs and for (b) $I=10^{14}$ W/cm^2 at time=14.3 fs. The units of $S(E)$ are arbitrary; peak values for all plots were set to 1.

W/cm^2, for which we expect stabilization to occur from the dressed-state model [9,10]. The dotted lines represent the two-surface ($1\sigma_g, 1\sigma_u$) calculations [9,10] (i.e., without ionization) of P_D, $f_1(R)$ and of the H and H^+ spectra, whereas the dashed lines in Fig. 1 represent P_6 resulting from the two-surface model. We observe in general a reasonable agreement between our exact calculations and the two-surface calculations for the intensity $I=3.5\times10^{13}$ W/cm^2, despite the fact that the ionization probability P_I at $I=3.5\times10^{13}$ W/cm^2 after $t=20$ fs is already equal to 0.14. However, at $I=10^{14}$ W/cm^2 our results are very different from the two-surface calculations. The probability of ionization already at $t=15$ fs is equal to 0.38. This means that it will be difficult to observe the stabilization at this intensity. From these figures (1–3) we observe two signatures of molecular stabilization:

(a) The population of the initial state ($v=6$ state in our case) stops to be depleted and grows after $t=10$ fs for $I=3.5\times10^{13}$ W/cm^2 [Fig. 1(a)]. For $I=10^{14}$ W/cm^2 [Fig. 1(b)] this growth is still visible but is much less than predicted by the two-surface model, because of the fast ionization process. This population growth is obviously related to the stimulated emission process which is the main origin of the molecular stabilization. The electronic Rabi frequency $d\varepsilon_0/h=R\varepsilon_0/(2h)$ is about 2×10^{14} s^{-1}, for $R=2$ bohrs, at 3.5×10^{13} W/cm^2, which is larger than the ionization rate (Table II).

TABLE II. H_2^+ ionization rates Γ (10^{12} s^{-1}) from the full 3D dynamical model and $\Gamma(R)$ from the model with frozen R [6,7].

I (W/cm^2)	Γ ($v=6$)	Γ (H atom)	Γ ($R=6$)	Γ ($R=11$)
3×10^{13}	4.4	0.20	5.5	1.8
10^{14}	32.8	49	47	10

(b) The plots of probability distributions of nuclear fragments $f_1(R)$ [Figs. 2(a) and 2(b)] show the formation of two sharp peaks near 3 and 3.6 bohrs. These peaks occur at the *turning points* of the nuclear motion on the upper adiabatic electronic potential created by the laser-induced avoided crossings between dressed $1\sigma_g$ and $1\sigma_u$ surfaces [2,9,10]. The shape of these peaks varies little as a function of time for $I=3.5\times10^{13}$ W/cm^2, while for $I=10^{14}$ W/cm^2 the peaks are formed at $t=8$ fs but for $t=15$ fs they already are strongly decreased by the ionization. The situation is very different for $I=7.5\times10^{12}$ W/cm^2 for which no clear peaks were found and the shape of $f(R)$ resembles the probability of the initial $v=6$ state. At this lower intensity, the dressed-state model predicts maximum dissociation, i.e., no stabilization from the laser-induced avoided crossing mechanism.

The kinetic-energy spectra of the dissociating products shown in Figs. 3(a) and 3(b) do not differ much from two-surface calculations for the lower intensities, 7.5×10^{12} and 3.5×10^{13} W/cm^2. These spectra have a strong maximum around 4.6 eV that can be attributed to the direct $1\sigma_g\rightarrow1\sigma_u$ one-photon dissociation from the $v=6$ vibrational state (4.58 eV). For the higher intensity, $I=10^{14}$ W/cm^2, this peak becomes broader than for the previous lower intensities, and additional plateaus at energies between 6 and 8 eV are being formed. We emphasize that the spectrum in Fig. 3(b) is calculated at a very early time, when the bound-state part and outgoing wave part of the nuclear wave function are not well separated. Longer time simulations up to 26 fs with a linear turn-off of the pulse of 1 fs were also performed. The resulting spectra and probabilities $f(R)$ ($|z|<z_{\max}$), $f_1(R)$ ($|z|<z_I$) are shown in Figs. 4 and 5, respectively. Clearly, the outgoing part of the wave function is already well separated from the bound part ($R<R_D$). The kinetic-energy plateau that is seen in Fig. 3(b) becomes bigger for later times, and several distinct peaks at 5.2, 5.8, 6.7, 7.7, 8.6, and 9.6 eV can be seen in Fig. 5. Since our simulation used the initial $v=6$ state, if Coulomb explosion occurs via a direct $\sigma_g\rightarrow\sigma_u$ transition, then one would expect to see the released energy equal to $e/(2.7a_0)=10.1$ eV ($2.7a_0$ is the distance at which the nuclear wave packet is created by a resonant one-photon transition). We emphasize that there is no such peak in Figs. 3 and 5. All our spectra exhibit a sharp cutoff around 9–10 eV. Clearly Coulomb explosions occur at larger R distances with lower kinetic energies.

It is further possible that the explosions occur at the peak coordinates (3.0 and 3.6 bohrs) of the $f(R)$ plots. These explosions would release energies $e^2/3.6a_0=7.5$ and $e^2/3a_0=8.9$ eV. In other words, these explosions occur at the turning points (3 and $3.6a_0$) of the adiabatic potential well created by the laser-induced avoided crossings [2,8–10]. Such a mechanism has been currently invoked in Coulomb explosions of diatoms [13]; the measured kinetic-energy re-

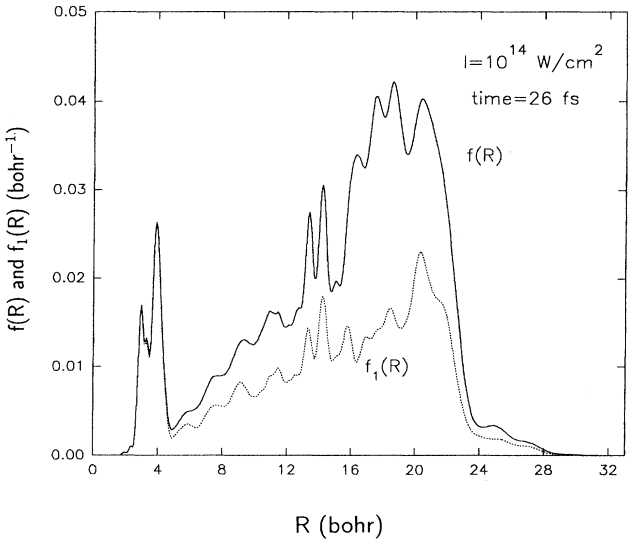

FIG. 4. Probability densities $f_1(R)$ and $f(R)$ for finding the protons in R defined by formulas (6) and (8) calculated at the end of the 26-fs pulse, with a linear turn-on and turn-off ramp of 1 fs, for $I=10^{14}$ W/cm^2.

leases of highly charged fragments are then systematically 70% of those expected from a simple Coulomb explosion energies occurring at the initial molecular equilibrium internuclear distance R_e.

Before attempting to find another interpretation for the observed spectra, let us compare our molecular ionization rates to the corresponding hydrogenic rates. We have noticed that the ionization probability P_I of H_2^+ from the vibrational $v=6$ state (the molecule is considerably stretched in this state; the $v=6$ right turning point is at $R=4.0$ bohrs compared to the equilibrium distance 2 bohrs) is much larger

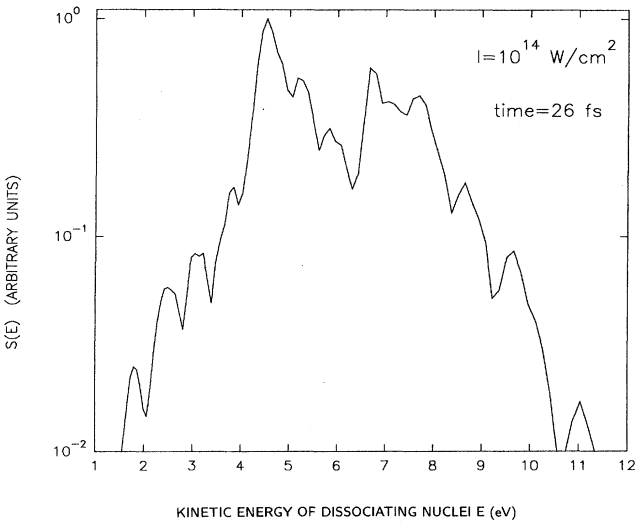

FIG. 5. Spectra of outgoing protons as functions of their relative kinetic energy E calculated at the end of the 26-fs pulse with a linear turn-on and turn-off ramp of 1 fs for $I=10^{14}$ W/cm^2. Units are arbitrary; peak values for all plots were set to 1.

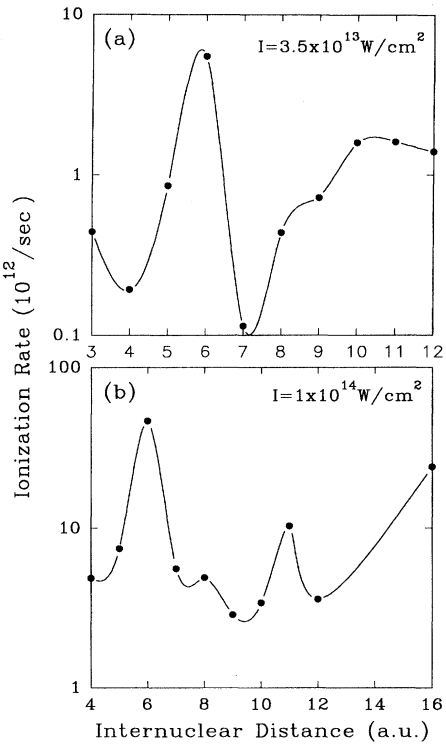

FIG. 6. Ionization rates of H_2^+ as functions of R calculated in the model with frozen nuclear motion [6,7] for (a) $I=3.5\times10^{13}$ W/cm^2; (b) $I=10^{14}$ W/cm^2.

than that for the H atom: $P_I^{H_2^+}(v=6)=0.1$, $P_I^H=0.003$ at $I=3.5\times10^{13}$ W/cm^2 at time $t=17$ fs, whereas for $I=10^{14}$ W/cm^2 the corresponding P_I's are $P_I^{H_2^+}$ $(v=6)=0.52$, $P_I^H=0.16$ for the same time. The corresponding ionization rates are listed in Table II. These are very surprising results since the ionization potential of H_2^+ frozen even at $R=4$ a.u. (the classical turning point for $v=6$) is much larger ($E_I=0.7$ a.u.) than the hydrogenic ionization potential (0.5 a.u.). The above-mentioned enhancement of ionization of stretched molecules seems to be a general phenomenon occurring both for short and long wavelengths and in a wide intensity range [16,17]. We have observed and rationalized this previously as being due to the presence of resonant charge-transfer states that have diverging transition moments [7]. Recent 1D models of highly charged diatoms show a similar enhancement of ionization for large distances [16,17]. In order to understand this phenomenon better, we have calculated ionization rates of H_2^+ as functions of R in the model in which the nuclei are frozen [6,7]. The results for both intensities, $I=3.5\times10^{13}$ W/cm^2 and $I=10^{14}$ W/cm^2 are shown in Figs. 6(a) and 6(b), respectively. In both figures we observe very strong peaks at two critical internuclear distances, $R_1=6$ a.u. and $R_2=11$ a.u. The first is a three-photon resonance to the ionization threshold, whereas the second seems to be correlated to a tunneling resonance. The ionization rates at these critical points are indeed close to those obtained from the present full dynamical model; seeTable II. For $I=3.5\times10^{13}$ W/cm^2 the ionization rates at R_1 and R_2 exceed the hydrogenic rates by a factor 25 and 9,

TABLE III. Energies of protons E_{expl} calculated as Coulomb explosions from $R_i=6$ or $R_i=11$ a.u. using the formula (9) compared with the energy peaks E_{spec} (eV), seen in Fig. 5. R_0 is the initial position of the $1\sigma_u$ nuclear wave packet.

R_0	R_i	E_{expl}	E_{spec}
2.73	6	9.1	9.6
2.73	11	7.05	6.7
3.0	6	7.8	7.7
3.0	11	6.05	5.8
3.6	6	6.4	6.7
3.6	11	4.6	4.5[a]

[a]Overlaps with the direct one-photon transitions process.

respectively, while for $I=10^{14}$ W/cm^2 those rates are of the same order as for the H atom (see Table II).

If the electrons are ejected at these maximum ionization distances R_i $(i=1,2)$ the corresponding kinetic energies of protons should be equal to e^2/R_i plus the energy acquired by $H+H^+$ sliding down from an initial R_0 to $R=R_i$ on the $1\sigma_u$ surface, i.e., if we neglect the laser field contribution to the experimental released energy we will obtain the explosion energies

$$E_{\text{expl}}=E_u(R_0)-E_u(R_i)+e^2/R_i, \quad i=1,2. \tag{9}$$

R_0 is the internuclear distance at which the wave packet sliding down the $1\sigma_u$ surface is initially created. The initial most probable value for R_0 is the distance at which the nuclear wave packet is created by the resonant one-photon transition $R_0=2.73$ a.u. This leads to the following values for explosion energies E^i_{expl}, $i=1,2$, $R_1=6$ or $R_2=11$ a.u.:

$$E^1_{\text{expl}}=9.1 \text{ eV}, \quad E^2_{\text{expl}}=7.05 \text{ eV}.$$

We can also suppose that the wave packet starts to slide down at R_0 equal to one of the maximum of the $f_1(R)$ plots, $R_0=3$ or $R_0=3.6$ (i.e., the turning points created by the laser-induced avoided crossing). This would lead to the following peaks:

$$E^1_{\text{expl}}=7.8 \text{ eV}, \quad E^2_{\text{expl}}=6.05 \text{ eV} \quad \text{for } R_0=3,$$

$$E^1_{\text{expl}}=6.4 \text{ eV}, \quad E^2_{\text{expl}}=4.59 \text{ eV} \quad \text{for } R_0=3.6.$$

All these possibilities are listed in Table III. We note that all the predicted kinetic energies from this simple model, described by (9), agree well with the peak positions resulting from the present three-body simulations; see Fig. 4 and Table III. We also note that a simple formula similar to (9) correctly predicts [17] the kinetic energies of highly charged fragments of Cl_2 observed in recent experiments [13], thus confirming the present mechanism of rapid ionization at large distances.

In all our spectra, Figs. 3 and 5, a series of low-energy peaks are seen ($E<4.5$ eV). These are also seen in two-surface calculations (dotted lines in Fig. 3 and the figures in Ref. [9]). It was shown in Ref. [9] that they originate from direct dissociation from lower vibrational states, $v=5,6,4\ldots$. These are populated due to the nonadiabatic effects (short-pulse rise and short duration of the pulse).

IV. CONCLUSION

A full dynamical calculation has been performed for H_2^+ in order to study competition between dissociation, ionization, and Coulomb explosion. Previous dressed-state models [2,9–11] of intense field photodissociation of H_2^+ has emphasized the importance of laser-induced avoided crossings and the creation of new laser-induced adiabatic potentials in describing the photodissociation dynamics. Our calculations show that stabilization of laser-induced vibrationally trapped states can be observed at intensities of about 10^{13} W/cm^2 and times shorter than 50 fs, but these are destroyed at higher intensities by competing ionization.

The signature of the laser-induced adiabatic potentials is clearly visible in the proton distribution functions $f_1(R)$ and $f(R)$, Figs. 2 and 4. The turning points of these laser-induced adiabatic potentials induce temporary vibrational trapping and show up as peaks in the proton densities $f(R)$. Kinetic-energy spectra of the photo-products exhibit maxima due to direct $(1\sigma_g \rightarrow 1\sigma_u)$ resonant photodissociation, Coulomb explosions from the laser-induced adiabatic turning points, and Coulomb explosions occurring at large internuclear distances R. Calculated ionization rates of H_2^+ at fixed R show that these rates have maxima at large distances, i.e., at around 6 and 11 a.u. These rates are shown to agree with those derived from the full dynamical ionization probabilities and thus explain the propensity for H_2^+ to produce Coulomb explosion fragments H^+H^+ with much lower kinetic energies than as would occur in direct, vertical (frozen R) Coulomb explosion. The calculated Coulomb explosion kinetic-energy peaks based on a simple model of explosions occurring at the turning points of laser-induced adiabatic potentials and at the predicted internuclear distance of maximum ionization rates reproduce well the full dynamical spectra (Table III). Recent experimental results by Schmidt, Normand, and Cornaggia have emphasized this phenomenon of the production of low kinetic-energy Coulomb explosion fragments [13]. Our calculations indicate that two mechanisms can produce such an effect. (i) laser-induced vibrational trapping, and (ii) enhanced ionization rates at certain large internuclear distances R.

In both mechanisms, Coulomb explosions (or even a sequence of Coulomb explosions of highly charged fragments, such as in the case of Cl_2 [13,17]) occur at larger R than the initial equilibrium distances, thus resulting in less energetic fragments [17].

ACKNOWLEDGMENTS

We wish to thank the Natural Sciences and Engineering Research Council of Canada for financing this research. We acknowledge also the support by Cooperation France-Quebec, ESR Contract No. 010392. We are very grateful to E. E. Aubanel for providing us with the results of two-surface H_2^+ calculations and discussions.

[1] J. H. Eberly, J. Javanainen, and K. Rzazewski, Phys. Rep. **204**, 331 (1991).

[2] *Molecules in Laser Fields*, edited by A. D. Bandrauk (Marcel Dekker, Inc., New York, 1994).

[3] J. H. Eberly, Q. Su, and J. Javanainen, Phys. Rev. Lett. **62**, 881 (1989); M. Horbatsch, Phys. Rev. A **44**, R5346 (1991).

[4] J. L. Krause, K. J. Schafer, and K. C. Kulander, Phys. Rev. A **45**, 4998 (1992).

[5] J. L. Krause, K. J. Schafer, and K. C. Kulander, Chem. Phys. Lett. **178**, 573 (1991); H. Wiedemann and J. Mostowski, Phys. Rev. A **49**, 2719 (1994).

[6] S. Chelkowski, T. Zuo, and A. D. Bandrauk, Phys. Rev. A **46**, R5342 (1992).

[7] T. Zuo, Z. Chelkowski, and A. D. Bandrauk, Phys. Rev. A **48**, 3837 (1993).

[8] A. D. Bandrauk and M. L. Sink, Chem. Phys. Lett. **57**, 569 (1978); J. Chem. Phys. **74**, 1110 (1981); A. Giusti-Suzor and F. H. Mies, Phys. Rev. Lett. **68**, 3869 (1992).

[9] E. E. Aubanel, A. D. Bandrauk, and P. Rancourt, Chem. Phys. Lett. **197**, 419 (1992); E. Aubanel, J. M. Gauthier, and A. D. Bandrauk, Phys. Rev. A **48**, 2145 (1993).

[10] E. E. Aubanel, A. Conjusteau, and A. D. Bandrauk, Phys. Rev. A **48**, R4011 (1993).

[11] J. W. J. Verschuur, L. D. Noordam, and H. B. van Linden van den Heuvel, Phys. Rev. A **40**, 4383 (1989); P. H. Bucksbaum, A. Zariyev, H. G. Muller, and D. W. Schumacher, Phys. Rev. Lett. **64**, 1883 (1990); Phys. Rev. A **42**, 5500 (1990); S. W. Allendorf and A. Szöke, *ibid.* **44**, 578 (1991); A. Zavriyev, P. H. Bucksbaum, J. Squier, and F. Salin, Phys. Rev. Lett. **70**, 1077 (1993).

[12] P. Dietrich, D. T. Strickland, M. Laberge, and P. Corkum, Phys. Rev. A **47**, 2305 (1993); D. Normand, L. A. Lompré, and C. Cornaggia, J. Phys. B **25**, L497 (1992).

[13] M. Schmidt, D. Normand, and C. Cornaggia, Phys. Rev. A **50**, 5037 (1994), and references therein; L. J. Frasinski, M. Stankiewicz, P. A. Hatherly, G. M. Cross, K. Colding, A. J. Langley, and W. Shaikh, *ibid.* **46**, R6789 (1992); W. T. Hill III, J. Zhu, D. L. Hatten, Y. Cui, J. Goldhar, and S. Yang, Phys. Rev. Lett. **69**, 2646 (1992).

[14] J. R. Hiskes, Phys. Rev. **122**, 1207 (1961).

[15] M. D. Feit, J. A. Fleck, Jr., and A. Steiger, J. Comput. Phys. **47**, 412 (1982); H. Shen and A. D. Bandrauk, J. Chem. Phys. **99**, 1185 (1993).

[16] P. B. Corkum, M. Ivanov, and T. Seidelman (private communication).

[17] S. Chelkowski, T. Zuo, and A. D. Bandrauk (unpublished).